



Theoretical Investigations into the Effects of Electric Field on Hydroxylamine Cation

Liu JIANGUO^{1,*}, An ZHENTAO¹, Zhang QIAN¹, Shi JINWEI¹, Wang CHAOYANG²

¹ Department of Ammunition Engineering, Ordnance Engineering College, Shijiazhuang, 050003, China

² School of Chemistry and Environment, South China Normal University, Guangzhou, 510006, China

Article Info

Received: 18/09/2016

Revised: 20/11/2016

Accepted: 25/12/2016

Keywords

Hydroxylamine cation
Electric field
Density functional theory
Energy level distribution
Field-assisted
dissociation

Abstract

In order to study the effect of the electric field on the propellant, geometry and charge distribution of NH_3OH^+ were optimized using density functional theory (DFT)/B3LYP at 6-311++G(d, p) basis set level under different external electric fields. Vertical ionization potential, adiabatic ionization potential, energy levels and HOMO-LUMO gap were calculated. And H^+ -loss dissociation reaction of NH_3OH^+ was studied. The results showed that the geometry, charge distribution and ionization potential were obviously dependent on electric field intensity. In the negative direction, with the increasing of the electric field intensity, the energy gap and dissociation reaction barrier were proved to decrease. And the dissociation of NH_3OH^+ became easier to occur.

1. INTRODUCTION

Hydroxylamine nitrate-based liquid propellant is a new type of environmental protection propellant ^[1]. As an ideal fuel for the liquid rocket engine, the propellant has edges of great density, high specific impulse, low freezing point, safe and nontoxic ^[2-5]. What's more, it is also widely used in aerospace field of micro and small propellant thrust system ^[6-8].

Electric ignition is usually adopted in the use of hydroxylamine nitrate-based liquid propellant. In the procession of ignition, an electric field always exists in the surface of the electrode. The effect of the electric field on the propellant has rarely been reported. ^[9] There are abundant hydroxylamine cations (NH_3OH^+) in the hydroxylamine nitrate-based liquid propellant. Thus, investigating into the effect of external electric field on NH_3OH^+ will provide a necessary theoretical support for the study of the effect of electric field on the propellant.

2. THEORY AND CALCULATION METHOD

The hamiltonian H of the molecular system under the external electric field can be expressed as ^[10]

$$H = H_0 + H_{\text{int}} \quad (1)$$

where H_0 is the hamiltonian of the molecular system without external fields, H_{int} is the hamiltonian of the interaction between electric field and molecular system. In the vicinity of a dipole, the hamiltonian of the interaction between electric field F and molecular system can be described in the following formula.

$$H_{\text{int}} = -\mu \cdot F \quad (2)$$

where μ is the molecular dipole distance.

Molecular structure of NH_3OH^+ without action of external electric field was shown in Fig.1. Along the direction of the Z axis, the external electric field varying from -0.005a.u. to 0.002a.u. was applied. And the

*Corresponding author, e-mail: 1729335676@qq.com

molecular structure of NH_3OH^+ could be optimized using density functional theory (DFT)/B3LYP at 6-311++G (d, p) basis set level. The vibration analysis of the optimized configuration was carried out. There was no virtual frequency in the calculation results showing that the optimized configuration was stable [11]. Adiabatic ionization potential (AIP) is the energy difference between ion optimization configuration and molecule optimization configuration. Vertical ionization potential (VIP) is the energy difference between molecule and the ion which has same optimization configuration but with a positive charge.

The geometries of the reactants, products, and transition states (TS) of H^+ -loss dissociation reaction were calculated with B3LYP/6-311++G (d, p) methods. The correlation between reactants, transition states and products would be confirmed by performing the intrinsic reaction coordinates (IRC) calculations. The dissociation reaction barrier of NH_3OH^+ were calculated with the zero-point energy (ZPE) correction. All the calculations were carried out using Gaussian 09.

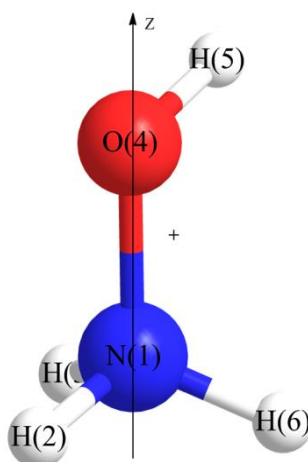


Figure 1. Molecular structure of hydroxylamine cation without action of external electric field

3. RESULTS AND DISCUSSION

3.1. Geometric configurations of hydroxylamine cation

Geometric parameters of NH_3OH^+ were shown in Tab.1-2 at different external electric field, and NH_3OH^+ all belonged to C_1 point group. According to the data from Tab.1-2, there was an obvious dependency relationship between geometric parameters of NH_3OH^+ and the intensity of electric field. The bond length R (1, 2) and R (1, 4) decreased with the increasing of electric field intensity. Varying the electric field increasing from -0.005a.u. to 0.002a.u., the bond length R (1, 2) decreased from 0.10316nm to 0.10284nm, and the bond length R (1, 4) decreased from 0.14072nm to 0.14056nm. Moreover, the bond length R (1, 4) decreased smoothly all the time. However, the bond length R (1, 2) decreased sharply from 0.10312nm to 0.10289nm with the electric field increasing from -0.001a.u. to 0.000a.u..

In general, the bond length R (1, 3), R (4, 5) and R (1, 6) increased with the increasing of electric field intensity. The bond length R (1, 3) almost remained unchanged in the negative electric field direction. But, there will be an apparent change in the bond length R (1, 3) with the reversing of the field direction. The bond length R (4, 5) increased smoothly in the negative electric field direction. However, it showed a linear growth in the positive electric field direction from 0.000a.u. to 0.002a.u.. The bond length R (1, 6) showed a linear growth in the negative electric field direction. Yet, it almost remained in the positive direction.

Table 1. The bond length of NH_3OH^+ under different external electric fields (R/nm)

F/a.u.	R (1,2)	R (1,3)	R (1,4)	R (4,5)	R (1,6)
-0.005	0.10316	0.10288	0.14072	0.09743	0.10307
-0.004	0.10315	0.10288	0.14068	0.09744	0.10308
-0.003	0.10314	0.10288	0.14065	0.09744	0.10309

-0.002	0.10313	0.10288	0.14062	0.09745	0.10310
-0.001	0.10312	0.10288	0.14059	0.09746	0.10310
0.000	0.10289	0.10311	0.14058	0.09746	0.10311
0.001	0.10286	0.10311	0.14057	0.09749	0.10311
0.002	0.10284	0.10312	0.14056	0.09752	0.10311

The bond angle increased with the growth of electric field. The bond angle A (2, 1, 3) and A (1, 4, 5) increased smoothly. While the bond angle A(3, 1, 4) increased sharply from 104.80° to 112.36° with the electric field changing from -0.001 a.u. to 0.000 a.u. The dihedral angle D(2,3,1,4) decreased smoothly with the increasing of electric field. However, the dihedral angle D(2,1,4,5) increased sharply from 56.568° to 179.967° when the field direction changed. And Fig.2 showed the molecular structure of NH_3OH^+ under different external fields.

Table 2. The bond angle and dihedral angle of NH_3OH^+ under different external electric fields (A/($^\circ$), D/($^\circ$))

F/a.u.	A (2,1,3)	A (3,1,4)	A (1,4,5)	D(2,3,1,4)	D(2,1,4,5)
-0.005	108.10	105.11	107.35	120.98	47.525
-0.004	108.14	105.01	107.36	120.80	50.592
-0.003	108.19	104.92	107.38	120.63	53.607
-0.002	108.24	104.85	107.40	120.46	56.593
-0.001	108.30	104.80	107.42	120.30	59.568
0.000	108.36	112.36	107.44	115.27	179.967
0.001	108.36	112.41	107.45	115.25	179.383
0.002	108.37	112.46	107.46	115.24	178.789

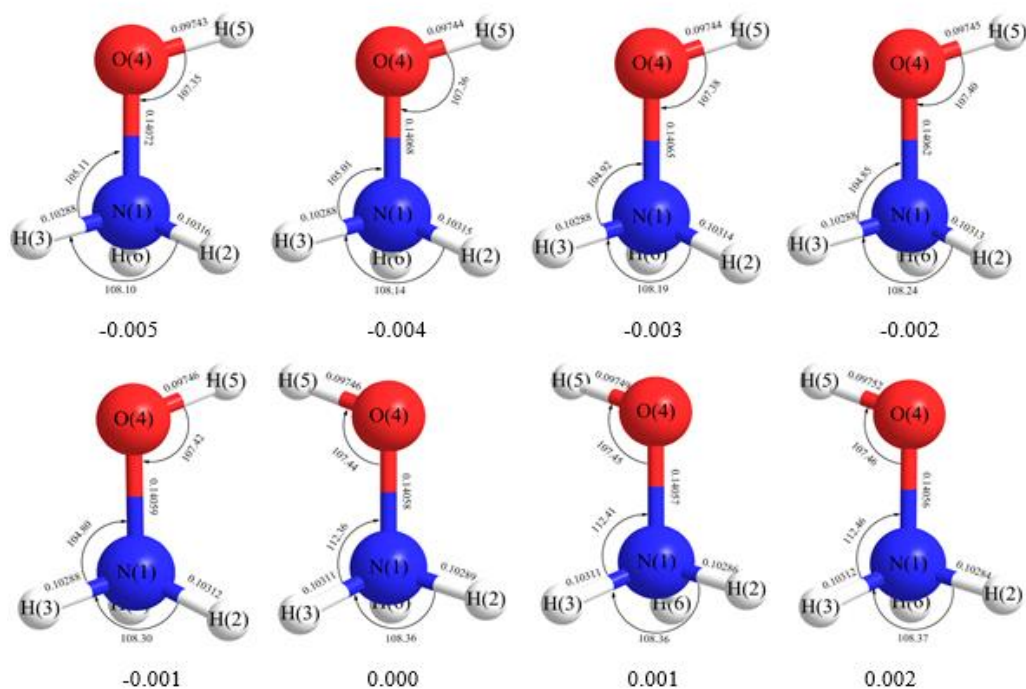


Figure 2. Molecular structure of hydroxylamine cation under different external electric field

3.2 Charge distribution of hydroxylamine cation

The variation of geometric parameter can be interpreted as the redistribution of the charge and electrostatic interaction under the action of electric field [12]. Tab.3 listed the charge distribution of NH_3OH^+ at different external electric fields. N and H atoms carried negative and positive electric charge, respectively. And O atom behaved electronegativity. Along with the growth of external electric field, the charge-transfer led to the increasement of electrostatic field intensity between N1 and H2 atoms. It also implied the attractive forces between two atoms became stronger. And moreover, the bond length R(1, 2) decreased with the rising of electric field. Contrary to the increasement of electrostatic field intensity between N1 and H2 atoms, the intensity between N1 and O4 atom decreased. That implied the repulsive force between two atoms became weaker. As a result, the bond length R (1, 4) got shorter. In addition, the electrostatic field intensity between N1 and H6 atom, O4 and H5 atom decreased with the increasing of external electric field. The weaker attractive forces between these two-atom led to the increasement of the bond length R (4, 5) and R (1, 6).

Table 3. The charge distribution of NH_3OH^+ under different external electric fields

F/a.u.	-0.005	-0.004	-0.003	-0.002	-0.001	0.000	0.001	0.002
N1	-0.4006	-0.3994	-0.3985	-0.3979	-0.3976	-0.3977	-0.3978	-0.3979
H2	0.3781	0.3753	0.3727	0.3701	0.3677	0.3979	0.3950	0.3921
H3	0.3957	0.3961	0.3965	0.3970	0.3974	0.3654	0.3667	0.3681
O4	-0.0612	-0.0590	-0.0569	-0.0547	-0.0526	-0.0504	-0.0523	-0.0542
H5	0.3214	0.3209	0.3204	0.3200	0.3197	0.3195	0.3222	0.3250
H6	0.3666	0.3661	0.3658	0.3655	0.3654	0.3653	0.3661	0.3670

3.3 Effect of electric field on vertical ionization potential and adiabatic ionization potential

At 6-311++G(d, p) basis set level and with the zero-point energy (ZPE) correction, the VIP and AIP of NH_3OH^+ at different external electric fields could be obtained utilizing density functional theory (DFT)/B3LYP. And the calculation results were shown in Tab.4. There was an obvious dependency relationship between the ionization potential and intensity of electric field. With the increasement of external electric field, the AIP showed the tendency of approximately linear decreasing. With the electric field increasing from -0.005a.u. to 0.002a.u., the AIP decreased from 4.6069eV to 4.5182eV.

Table 4. Adiabatic ionization potentials and vertical ionization potentials of NH_3OH^+ with different external electric fields

F/a.u.	-0.005	-0.004	-0.003	-0.002	-0.001	0.000	0.001	0.002
AIP/eV	4.8401	4.8222	4.8064	4.7933	4.7835	4.7770	4.7539	4.7446
VIP/eV	5.1792	5.1531	5.1250	5.0943	5.0605	5.0246	4.8464	4.8478
AIP+ Δ ZPE/eV	4.6069	4.5857	4.5676	4.5532	4.5430	4.5366	4.5313	4.5182
VIP+ Δ ZPE/eV	4.9802	4.9531	4.9244	4.8934	4.8597	4.8238	4.6522	4.6527

Similarly, VIP showed a same tendency with the increasement of external electric field. There were also some differences between the VIP and AIP. With the electric field increasing from -0.005a.u. to 0.000a.u., the VIP decreased smoothly from 4.9802eV to 4.8238eV. And the vertical ionization potential decreased sharply from 4.8238eV to 4.6522eV with the reversing of the field direction. After that the variation of VIP was extremely small, then the value could be thought of no changes.

In conclusion, the ionization potential of NH_3OH^+ decreased with the increasing of external electric field, which implied the NH_3OH^+ became much easier to lose the electrons.

3.4 Effect of electric field on energy level distribution

The highest occupied molecular orbital (HOMO) energy E_H , the lowest unoccupied molecular orbital (LUMO) energy E_L , and energy gap E_G were shown in Tab.5. The energy gap could be expressed as

$$E_G = (E_L - E_H) \times 27.2 \text{ eV} \quad (3)$$

The HOMO energy level stood for the ability of losing electron. The higher HOMO energy level, the molecular was easier to lose electron. The energy gap reflected the ability of electron transition from the HOMO to the LUMO [13-14]. What's more, it represented the ability to involve in chemical reactions.

Table 5. The highest occupied molecular orbital, lowest unoccupied orbital and energy gap variation with external electric fields

F/a.u.	-0.005	-0.004	-0.003	-0.002	-0.001	0.000	0.001	0.002
E_H /a.u.	-0.58867	-0.58877	-0.58885	-0.58891	-0.58895	-0.58896	-0.58895	-0.58893
E_L /a.u.	-0.23872	-0.23861	-0.23853	-0.23846	-0.23841	-0.23838	-0.23837	-0.23837
E_G /eV	9.5186	9.5244	9.5287	9.5322	9.5347	9.5358	9.5358	9.5352

The change regulation of energy gap with the electric field was shown in Fig.3. with different external electric fields, Fig.4 illustrated the spatial distribution of the HOMO and the LUMO. With the increasing field intensity in the negative direction, the HOMO energy level increased, and the LUMO energy level had a contrary trend. According to Equ.3, the energy gap decreased with the increasement of the field intensity. While in the positive direction, the HOMO energy rised with the growth of the field intensity, but the LUMO energy almost remained the same value. Then the same conclusion could be obtained using Equ.3. In summary, enhancing the electric field intensity could promote the ability of NH₃OH+ participating in chemical reactions.

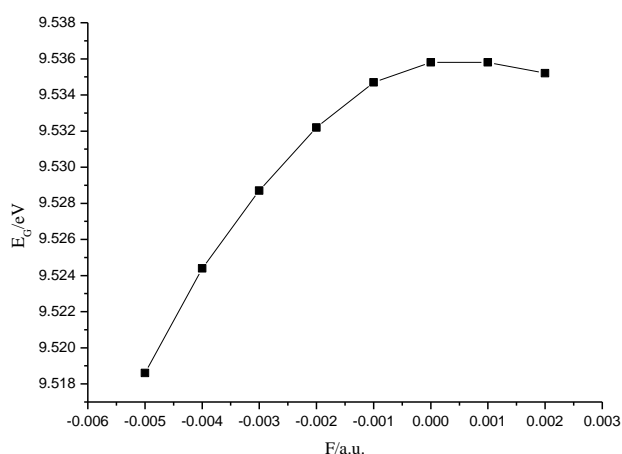


Figure 3. The energy gap variation with external electric fields

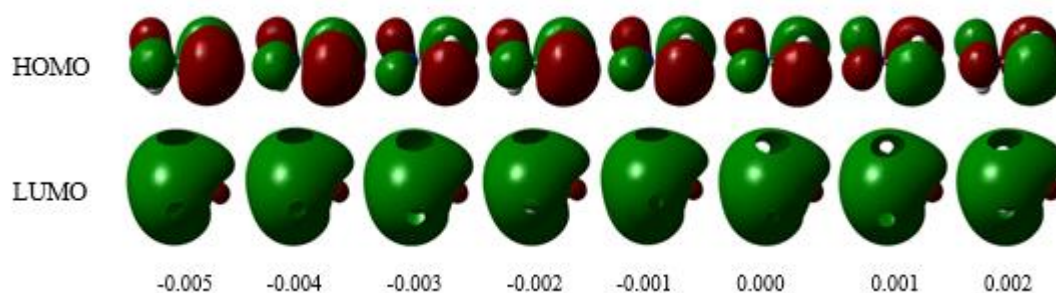


Figure 4. Frontier molecular orbital variation with external electric fields

3.5 Effect of electric field on H⁺-loss dissociation reaction

The barrier of dissociation reaction, geometry of transition state and charge of 6-H atom were calculated, and the calculation results were shown in Tab.6. Without the external electric field, the 6-H atom charge of products in H⁺-loss dissociation reaction was 1.0000e, which indicated the products of dissociation reaction were NH₂OH and H⁺. And the value of dissociation reaction barrier was 45.605kJ·mol⁻¹. Under the external electric field, the 6-H atom charge of products was equal to the former. Then the same conclusion could be obtained that the mechanism of NH₃OH⁺ dissociation under the electric field was identical with that without electric field. And the products of dissociation reaction were NH₂OH and H⁺.

With the electric field intensity rising from 0.001a.u. to 0.002a.u. in the negative direction, the barrier of dissociation reaction increased from 43.863kJ·mol⁻¹ to 53.711kJ·mol⁻¹. When the electric field varied from 0.002a.u. to 0.005a.u., the barrier sharply decreased from 53.711kJ·mol⁻¹ to 4.8429kJ·mol⁻¹. And it reduced more than 90%. While if the electric field intensity reached 0.006a.u., the transition state would disappear. That implied NH₃OH⁺ became unstable and dissociated to NH₂OH+H⁺ spontaneously. [15] In general, the NH₃OH⁺ became easier to dissociate with the increasing of the electric field intensity in the negative direction. In the positive direction, however, with the growth of the electric field intensity, the barrier of dissociation reaction did not change so much.

Table 6. The geometries of transition states (R/nm), energy barriers (ΔE /kJ·mol⁻¹) of dissociations reaction, and the charge values (Q (6-H)/e) on the 6-H atom in the products

F/a.u.	R (1,2)	R (1,3)	R (1,4)	R (4,5)	R (1,6)	ΔE	$\Delta E + \Delta ZPE$	Q (6-H)
NH ₃ OH ⁺ → NH ₂ OH+H ⁺								
-0.005	0.101737	0.102147	0.134766	0.097356	0.480105	7.4827	4.8429	1.0000
-0.004	0.101732	0.102136	0.134642	0.097382	0.486247	15.753	13.117	1.0000
-0.003	0.101728	0.102126	0.134523	0.097408	0.492128	50.200	47.643	1.0000
-0.002	0.101725	0.102116	0.134410	0.097435	0.497468	55.503	53.711	1.0000
-0.001	0.101724	0.102106	0.134304	0.097461	0.501644	46.340	43.863	1.0000
0.000	0.102098	0.101724	0.134204	0.097488	0.503840	48.125	46.605	1.0000
0.001	0.102095	0.101712	0.134098	0.097530	0.507343	47.495	44.916	1.0000
0.002	0.102093	0.101702	0.133998	0.097572	0.509295	49.149	47.219	1.0000

4. CONCLUSION

Density functional theory B3LYP at 6-311++G (d, p) basis set level was used to study the effect of electric field on the hydroxylamine cation. The study reached the following results:

- (1) The geometry and charge distribution of NH_3OH^+ depended on electric field intensity obviously. And the redistribution of the charge and electrostatic interaction under the action of electric field illustrated the variation of geometric parameter.
- (2) With the increasing of external electric field, the ionization potential of NH_3OH^+ decreased, and NH_3OH^+ became easier to lose electrons.
- (3) The energy gap dropped with the increasement of the electric field intensity, and the ability of hydroxylamine cation to participate in chemical reactions gained promotion.
- (4) And with rising of the electric field intensity in negative direction, the dissociation reaction barrier was proved to decrease, the dissociation of NH_3OH^+ became easier to occur. In the positive direction, however, with the increasing of the electric field intensity, the value of dissociation reaction barrier remained.

CONFLICT OF INTEREST

No conflict of interest was declared by the authors

REFERENCES

- [1] Amrousse, R., Katsumi, T., Niboshi, Y., Azuma, N., Bachar, A., Hori, K., "Performance and deactivation of Ir-based catalyst during hydroxylammonium nitrate catalytic decomposition", *Applied Catalysis A*, 452: 64-68, (2013).
- [2] Ulas, A., Boysan, E., "Numerical analysis of regenerative cooling in liquid propellant rocket engines", *Aerospace Science and Technology*, 24: 187-197, (2013).
- [3] Wei, J. B., Shaw, B. D., "Influences of pressure on reduced-gravity combustion of HAN-methanol-water droplets in air", *Combustion and Flame*, 146: 484-492, (2006).
- [4] Barney, G. S., Duval, P. B., "Model for predicting hydroxylamine nitrate stability in plutonium process solutions", *Journal of Loss Prevention in the Process Industries*, 24: 76-84, (2011).
- [5] Courthéoux, L., Amariei, D., Rossignol, S., Kappenstein, C., "Thermal and catalytic decomposition of HNF and HAN liquid ionic as propellants", *Applied Catalysis B: Environmental*, 62: 217-225, (2006).
- [6] Kim, H. J., Seo, S., Lee, K. J., Han, Y. M., Lee, S. Y., Ko, Y. S., "Stability rating tests for the length-optimization of baffles in a liquid propellant combustion chamber using a pulse gun", *Aerospace Science and Technology*, 12: 214-222, (2008).
- [7] Akira, K., Hiroyuki, K., Kimiya, K., Yoshihiro, A., "Design and performance of liquid propellant pulsed plasma thruster", *Vacuum*, 73: 419-425, (2004).
- [8] Koizumi, H., Kawazoe, Y., Komurasaki, K., Arakawa, Y., "Effect of solute mixing in the liquid propellant of a pulsed plasma thruster", *Vacuum*, 80: 1234-1238, (2006).
- [9] Milekhin, Y. M., Sadovnichii, D. N., Tyutnev, A. P., "Electrical effects in propellant compositions radiated by electrons", *Combustion, Explosion, and Shock Waves*, 43: 538-548, (2007).
- [10] Ghazi, H. E., Jorio, A., "Excited-states of hydrogenic-like impurities in InGaN-GaN spherical QD: Electric field effect", *Physica B*, 430: 81-83, (2013).
- [11] Alavi, S. and Thompson, D. L., "Effects of Alkyl-Group Substitution on the Proton -Transfer Barriers in Ammonium and Hydroxylammonium Nitrate Salts", *J. Phys. Chem. A*, 108: 8801-8809, (2004).
- [12] Du, J. B., Tang, Y. L., Long, Z. W., "Molecular structure and electronic spectrum of pentachlorophenol in the external electric field", *Acta Phys. Sin.*, 61: 153101-153107, (2012).

- [13] Sakai, T., Matsumoto, M., Okunishi, K., “Energy gap of spin nanotube”, *Physica E*, 29: 633-636, (2005).
- [14] Horwitz, L. P., Engelberg, E. Z., “Energy gaps in a spacetime crystal”, *Physics Letters*, 374: 40-43, (2009).
- [15] Chang, H. B., Chen, B. Z., He, Y. J., “A theoretical study for the highly charged cations of C₂H₂ with and without external electric fields”, *Acta Chimica Sinica*, 3: 308-314, (2008).